Synthetic Orbital Landing Area for Crater Elimination (SOLACE)

AggieSat Laboratory

Advisor: Dr. Helen Reed

Texas A&M University

Introduction

Plume surface interaction (PSI) is a major hindrance to the safety and success of future crewed missions to the lunar surface. Lunar landers are known to both remove local regolith from the landing site on descent and throw this ejecta away at high speeds, known as cratering and regolith dispersal, respectively.

Cratering and dispersal form unique challenges for lunar exploration and development. For one, both are extremely hard to study and characterize on Earth. As such, only poor estimates exist for important parameters such as the onset altitude of PSI and the relationship between lander mass and the magnitude of cratering and dispersal [1-2].

Additionally, systems such as *Surveyor III* (see right) and Curiosity sustained damage to their structures and sensors during Apollo 12's descent and the Mars Science Laboratory, respectively. Thus, for human landing systems (HLS), it is imperative that PSI be mitigated to protect the safety of the crew and vehicle [3-6].

Figure 1. Damage on Surveyor III camera shroud due to PSI. [4]

Objectives and Solution Overview

The proposed solution is a deployable, autonomous, artificial landing pad called SOLACE. For this concept, several primary and secondary objectives were developed.

Primary Objectives

- Act as a safe landing platform for HLS
- Reduce impact of lunar PSI on local infrastructure
- Monitor lunar PSI on descent, as well as for future landers

Secondary Objectives

- Retain the capability to act as a foundation for future lunar infrastructure

These objectives precipitated into a concept of operations (CONOPS). The CONOPS below begins with SOLACE in a Low Lunar Orbit (LLO).

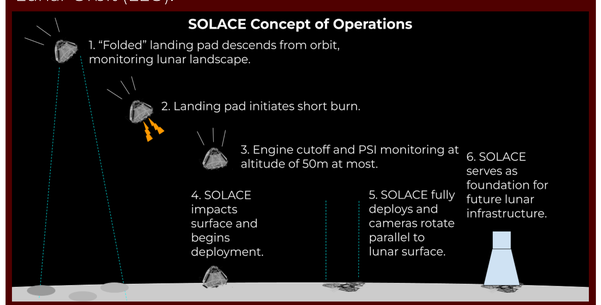

Figure 2. CONOPS of SOLACE from LLO.

System Design and Operations

An intensive trade study was performed to determine the optimal landing site for SOLACE. The optimal landing site was determined to be in the Haworth Landing region.

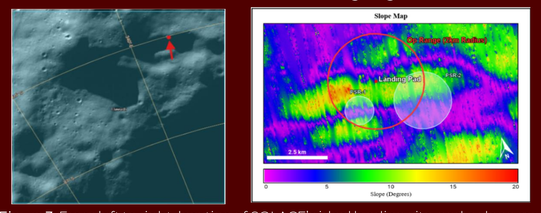

Figure 3. From left to right, location of SOLACE's ideal landing site, and a slope map of SOLACE's ideal landing site displaying an operational zone of 2 km.

Thermal, Mechanics, and Structures (TMS)

SOLACE uses a "bunker"-esque design. As seen below, it is made of a lower base, plume redirection system, grating section of the pad, main landing surface, and methalox-propelled thrusters. Spring-loaded actuators are responsible for fin deployment , as well as stakes into the lunar surface to secure SOLACE on HLS descent. SOLACE is primarily composed of graphene, titanium aluminide, and hafnium diboride. SOLACE is 1.4 m tall, occupies 18.28 m^3 of volume and has 9 m^3 available for other components

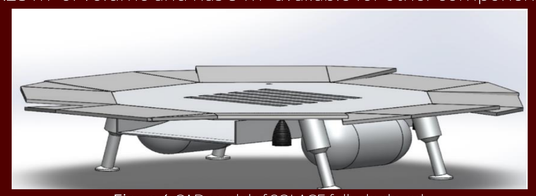

Figure 4. CAD model of SOLACE fully deployed.

Guidance, Navigation, and Control (GNC)

SOLACE's guidance subsystem uses a novel machine-learning algorithm that identifies safe landing zones on descent. This algorithm is trained from available video from previous lunar missions. The navigation system is comprised of the Honeywell HG1900 IMU, RocketLab's ST-16HV star tracker, RedWire's Coarse Sun Sensor, and NASA's Navigational Doppler LiDAR (NDL). SOLACE's trajectory can be seen in Figure 5 below.

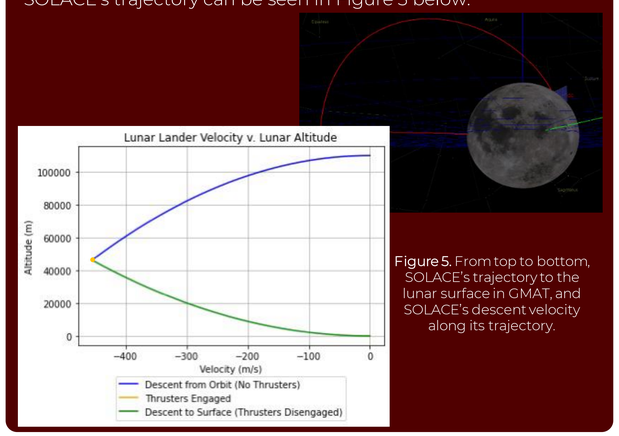

Figure 5. From top to bottom, SOLACE's trajectory to the lunar surface in GMAT, and SOLACE's descent velocity along its trajectory.

System Design and Operations (cont.)

Electrical Power Subsystem (EPS)

The EPS provides power generation, storage, and management to SOLACE. SOLACE employs two 7-cell lithium-ion batteries for power, and has a sensor suite consisting of the NDL, a ring laser gyro, accelerometer, and thermistor. These, with the rest of the system, result in an estimated power budget of 4794 W at Beginning Of Life (BOL). The EPS layout is shown below.

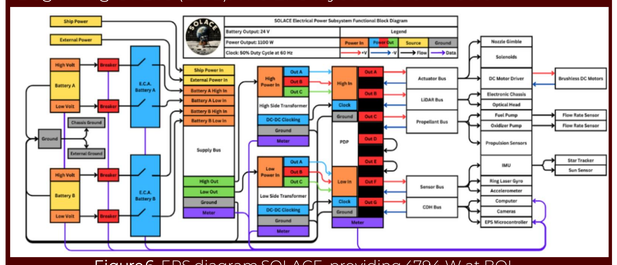

Figure 6. EPS diagram SOLACE, providing 4794 W at BOL.

Communications (COM)

SOLACE's communication subsystem utilizes the SRS-4 Full-duplex High-Speed S-band transceiver. Additionally, the center frequency was chosen to be 2250 MHz using 16-QPSK. Extensive research and trade studies were performed on regolith properties in conjunction with a thorough link analysis to finalize a design giving a maximum gain of 11 dBi. The selected antenna was the IQ-Spacecom S-band patch antenna.

Command and Data Handling (CDH)

The CDH subsystem uses an NVIDIA Jetson Orin AGX 64 GB alongside three ArduCam IMX586 48MP Camera Modules for flight computing and PSI monitoring. The CDH subsystem uses 3D particle tracking velocimetry for PSI measurement, focusing on particles larger than 20µm.

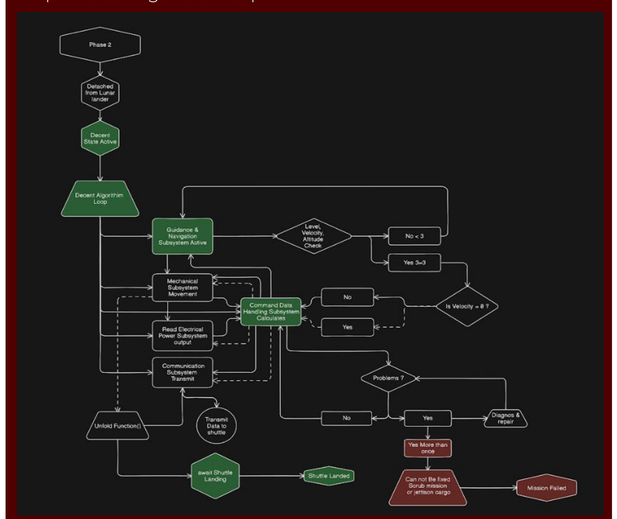

Figure 7. CDH HSM of SOLACE's in-flight phase.

System Merit and Recommendations

System Merit

- **Performance**: SOLACE adheres to all of HuLC's guidelines and constraints and succeeds in all its verification and validation test plans.
- **Technology Readiness**: SOLACE contains only TRL 9 technologies, requiring no technological development.
- **Risk**: SOLACE is a low-risk solution as landing pads are common and low in complexity, as shown in Figure 8.
- **Programmatic Implementation**: SOLACE is compatible with virtually any HLS vehicle or lunar region.
- **Cost**: From NASA's PCEC software, SOLACE is estimated to have an NRC of $168.1M FY2024 and a total program cost of $1944.9M FY2024.

Likelihood \ Severity	Insignificant	Minor	Moderate	Major	Severe
Almost Certain					
Likely			4		
Possible			2	5	1, 3
Unlikely		3f, 5f	1f		
Rare	4f	2f			

1: SOLACE detaches from surface

2: Accelerated degradation

3: Failed deploy

4: Brownout on descent

5: SOLACE departs from trajectory

Figure 8. Risk matrix of SOLACE's five most critical issues with values after mitigation.

Mitigation plans include adding stakes to the design, use of spring-loaded actuators, and robust regulation of electronics.

Recommendations

Some takeaways from SOLACE's development are as follows:

- SITE team was a major advantage
- Grating and ducting can be aerodynamically optimized
- Propulsion system was a design inhibitor

References

[1] C. Immer, J. Lane, P. Metzger, and S. Clements. "Apollo Video Photogrammetry Estimation of Plume Impingement Effects," Icarus, vol 214, p. 46-52, 01 2014.

[2] P.T. Metzger, J. Smith, and J.E. Lane, "Phenomenology of Soil Erosion due to Rocket Exhaust on the Moon and the Mauna Kea Lunar Test Site," Journal of Geophysical Research: Planets, vol 116, no. E6, 2011.

[3] J.R. Gaier, "The Effects of Lunar Dust on EVA Systems During the Apollo Missions," Tech. Rep. NASA/TM---2005-213610, Glenn Research Center, Cleveland, OH, Mar. 2005.

[4] P. Zanon, M. Dunn, and G. Brooks, "Current Lunar Dust Mitigation Techniques and Future Directions," Acta Astronautica, vol 213, pp. 627-644, 2023.

[5] J. Gómez-Elvira, et al. "Curiosity's Rover Environmental Monitoring Station: Overview of the First 100 Sols," Journal of Geophysical Research: Planets, vol 119, p. 1680-1688, July 2014.

[6] R.N. Watkins, et al. "Understanding and Mitigating Plume Effects During Powered Descents on the Moon and Mars," 2021.